

Fabrication of Conjugated Polymer Hybrid Thin Films with Radially Oriented Aluminosilicate Nanofibers by Spin-Assembly

Nattha Jiravanichanun,[1] Kazuya Yamamoto,[1] Hiroaki Yonemura,[2] Sunao Yamada,[2,3] Hideyuki Otsuka,*[1] and Atsushi Takahara*[1]

[1]Institute for Materials Chemistry and Engineering, Kyushu University, 744 Motooka, Nishi-ku, Fukuoka 819-0395

[2]Department of Applied Chemistry, Faculty of Engineering, Kyushu University, 744 Motooka, Nishi-ku, Fukuoka 819-0395

[3]Center for Future Creation, Kyushu University, 744 Motooka, Nishi-ku, Fukuoka 819-0395

Received June 11, 2008; E-mail: otsuka@ms.ifoc.kyushu-u.ac.jp, takahara@cstf.kyushu-u.ac.jp

Multilayer hybrid films of imogolite nanofibers and water-soluble poly(*p*-phenylene) (WS-PPP) were prepared by two assembly methods. Layer-by-layer (LBL) assembly and spin-assembly were applied to fabricate the hybrid films. The deposited amount of WS-PPP per thickness was not significantly different between the two methods. However, the spin-assembly method gave significant orientation of imogolite nanofibers aligned in the radial direction, while imogolite nanofibers were randomly networked in the LBL film. The results suggested that lyotropic mesophase of imogolite and centrifugal and shear forces influenced a self-assembly of imogolite fibers oriented in a force-inducing direction.

Spin-assembly techniques for polyelectrolytes have been energetically studied over the past decade to organize heterostructures on a substrate, especially thin films[1–10] utilizing electrostatic forces to facilitate the deposition process. This technique was developed from the basic layer-by-layer (LBL) assembly method for polyelectrolytes described by Decher et al.[11,12] Basic LBL assembly can be achieved by first dipping a substrate into cationic solution for a period of time, followed by rinsing with pure solvent. Without washing with pure solvent after adsorption of the polyelectrolyte layer, the weakly adsorbed polyelectrolyte chains increase the film roughness and thickness, yielding poor film quality. Before the next dipping step, a drying process is also necessary because a remaining water layer may disturb the adsorption of subsequent polyelectrolytes. Therefore, rinsing and drying steps are necessary and require careful preparation. The same substrate is then dipped into anionic solution, rinsed and dried. The process is then repeated from the beginning to make multilayer films. For spin-assembly, a spin-coating step is applied instead of a dipping step using a spin coater. During spinning, removal of weakly adsorbed polyelectrolytes and preadsorbed water molecules occurs simultaneously with polyelectrolyte adsorption.[13,14] Therefore, rinsing and drying steps are not necessary for the spin-assembly, which shortens the film preparation process. Additional advantages of spin-assembly over the conventional LBL assembly are improved time-efficiency, acceptable reproducibility and uniform coating in terms of the deposition amount.

Imogolite is a clay minerals contained in volcanic ash soils.[15,16] It is a hydrous aluminosilicate and has fibrous morphology and a diameter of approximately 2 nm (Figure 1a). The chemical structure demonstrates that the AlOH groups are exposed on the outer surface of the fiber, so the surface charge depends on the pH of the solution and maintenance of a positive charge at low pH. Therefore, imogolite are appropriately utilized with negative charged polymers for LBL assembly without modifying the fiber surface. Very importantly, imogolite can also be synthesized chemically from tetraethoxysilane and aluminum chloride.[17–19] Imogolite has been investigated in several applications such as membrane, catalyst, adsorbents, and improving the optical, thermal, or mechanical properties of polymers.[19–24] Surface modification,[25] porous film fabrication,[26] and self-assembly[27] of imogolite have also been reported.

We have focused on imogolite due to the high aspect ratio for a large surface area and the positively charged surface ability to bind to anionic polyelectrolyte. One of the most important properties of imogolite is its optical transparency. Hybrid films of imogolite and polymers with important optical properties are likely to be prepared. In contrast, the representative nanowire carbon nanotubes, will negate optical properties of a hybrid film due to their strong optical absorbance. Therefore, imogolite nanofibers were used as templates to assemble conjugated polymer at the surface of nanofibers by ionic interaction. We employed poly[disodium 2,5-bis(3-sulfonatopropoxy)-1,4-phenylene-*alt*-1,4-phenylene] (WS-PPP)[28] as an anionic polyelectrolyte, which is water-soluble and has a conjugated molecular structure. The chemical structure is shown in Figure 1a. As expected, imogolite and the WS-PPP mixture formed a gel even showing clear solution before mixing. This alteration indicated that there is an ionic interaction between WS-PPP and the surface of imogolite. Moreover, the increase in the WS-PPP content in mixture enhanced dispersion of imogolite fibers. These preliminary experimental results initiated

Published on the web December 12, 2008; doi:10.1246/bcsj.81.1663

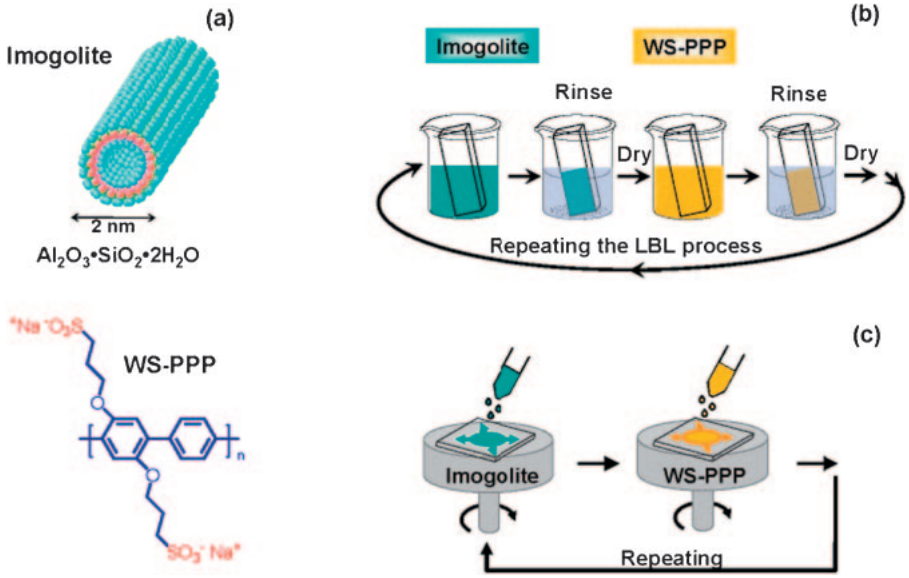

Figure 1. Schematic representation of the structure of imogolite and the chemical structure of WS-PPP (a). Schematic representation of the LBL assembly (b) and spin assembly (c).

an idea to fabricate an ordered layer assembly of imogolite and WS-PPP instead of the hybrid bulk matrix. In the present paper, we report the preparation of ultrathin multilayer hybrid films by applying two self-assembly methods. One is the LBL assembly and the other is the spin-assembly. The two assembly films were characterized by X-ray photoelectron spectroscopy (XPS) and UV–vis spectroscopy. The film thickness and surface topology were also observed by atomic force microscopy (AFM).

Experimental

Materials. Concentrated sulfuric acid and aqueous hydrogen peroxide solution were used for cleaning the substrates. 3-Mercaptopropyltrimethylsilane (MTS) and toluene were used in chemical vapor adsorption (CVA). Imogolite was synthesized by a previously reported method[19] and WS-PPP was used as received. The diameter of imogolite nanofibers was estimated to be ca. 2 and 10–15 nm for a bundle form by TEM. Sodium acetate and acetic acid were used to prepare acetate buffer pH 4 for the solvent of imogolite. Water in this experiment was purified with a Nanopure Water system, $\rho > 18\,\mathrm{M\Omega\,cm}$ (Millipore, Inc.). Silicon wafers and quartz plates were used as substrate.

Substrate Preparation. Substrates were cleaned in piranha solution at 100 °C for 1 h and rinsed with water. The substrates were then dried in vacuo and irradiated by vacuum ultraviolet ray (wavelength 172 nm) to remove organic contamination. The CVA process of MTS[29] was carried out by maintaining substrates in a sealed container at 100 °C for 2 h. After the heating treatment, substrates were immediately rinsed with toluene and dried in vacuo. The substrates were then irradiated by UV-light (wavelength 365 nm) for over 10 h in air in order to transform terminal mercapto groups to sulfonic acid groups.[30,31]

Multilayer Assembly Preparation. LBL Assembly Method (Figure 1b): Negatively charged substrates with sulfonic acid groups were immersed in imogolite solution (1 mM) and WS-PPP solution (1 mM) alternatively. The molar concentrations were calculated based on the repeating unit of each polyelectrolyte shown in Figure 1. The immersion times were 20 and 10 min, respectively, followed by 2 min of immersion in water after each dipping step. Substrates were dried in air after each rinsing step. The process was repeated from the beginning to make multilayer films.

Spin-Assembly Method (Figure 1c): Spin-assembly for one-bilayer consisted of: (1) dropping 0.5 mL of imogolite solution on the spinning, negatively charged substrates and spinning at 6000 rpm for 20 s, (2) rinsing with 2 mL of water during spinning, and (3) repeating step (1) for WS-PPP solution followed by the rinsing step. The process was repeated to make multilayer films.

Characterization. The presence of imogolite and WS-PPP in the hybrid films was identified by XPS with XPS-APEX (ULVAC PHI Co., Ltd.). The XPS measurements were performed with a monochromatized Al Kα X-ray source at 14 kV. The emission angle of the photo electrons was set to 45°. Light transmissions were measured with a UV–vis spectrometer, Lamda 35 (Perkin-Elmer Japan Co., Ltd.), at a wavelength region of 190 to 450 nm. The aromatic groups of WS-PPP allows $\pi \rightarrow \pi^*$ adsorption to be monitored by UV–vis spectroscopy. Polarized absorption spectra of the LBL and spin films were recorded on a UV–vis–NIR scanning spectrometer (Shimadzu UV-3150) using a polarizer (Assy II; 260–700 nm) and a sample-immobilization set of glass plates (Shimadzu P/N 206-81042) for the measurement of samples prepared on quartz plates.[32]

The intermittent contact-mode and contact-mode AFM observations were carried out using an SPA400 AFM head with an SPI4000 Probe Station (SII Nano Technology, Inc.) at room temperature. AC mode AFM used a Si_3N_4 integrated tip on a commercial rectangular cantilever (Olympus Co., Ltd) with a 108-μm length, a spring constant of $15\,\mathrm{N\,m^{-1}}$ and a resonant frequency of 160 kHz for surface topology observation. Contact mode AFM used a SiN integrated tip on a commercial rectangular cantilever (Olympus Co., Ltd) with a 200-μm length, a spring constant of $0.1\,\mathrm{N\,m^{-1}}$ and a resonant frequency of 19 kHz for thickness observation.

Results and Discussion

In the case of the LBL assembly and spin-assembly, the substrates for the preparation of hybrid films required some inter-

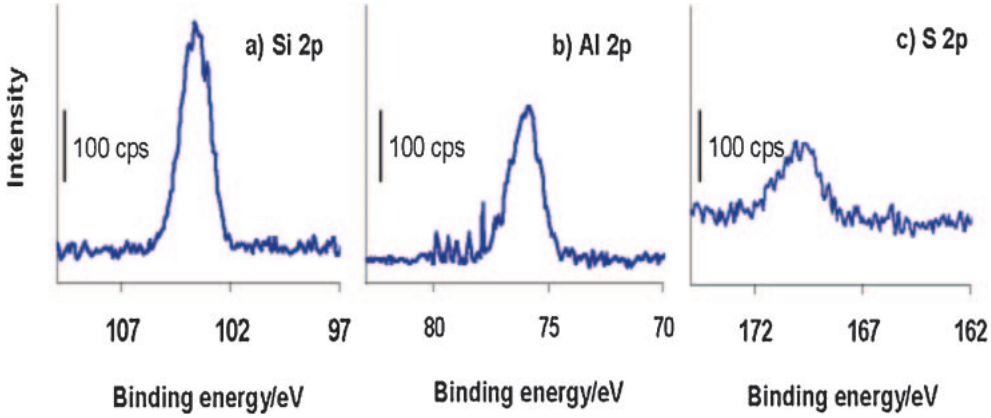

Figure 2. XPS peaks of the surface of 30 bilayers LBL film. a) Si 2p and b) Al 2p spectra of imogolite, and c) S 2p spectrum of WS-PPP.

action with the film component. The substrates were treated with MTS to prepare an organosilane monolayer with mercapto groups and subsequent oxidation was carried out to convert the mercapto group into a sulfonic acid group, which can form electrostatic interactions with the surface of imogolite.

Figure 2 shows the XPS spectra of a 30-bilayer film of imogolite and WS-PPP prepared by the LBL assembly method. The Si 2p and Al 2p peaks originating from aluminosilicate imogolite were observed at 103.6 and 75.8 eV, respectively. In addition, the S 2p peak was clearly observed at 169.7 eV, which demonstrated the incorporation of sulfonate groups of WS-PPP into the film. The presence of Si, Al, and S could be attributed to the successful fabrication of the imogolite/WS-PPP hybrid film on substrate. The XPS spectra of the film prepared by spin-assembly also appeared the same (data are not shown). XPS quantitative analyses were performed to determine the S/Al ratio of both hybrid films. The S/Al ratio reflects the composition of WS-PPP relative to the amount of imogolite. For the LBL film, the S/Al ratio was determined as 0.27, which is slightly higher than the value of 0.23 for the spin-assembly film.

UV–vis absorption spectra of the 15-bilayer hybrid films prepared by both assembly methods are shown in the inset of Figure 3. The conjugated aromatic system on WS-PPP absorbed light at λ_{max} of 345 nm, indicating the qualitative amount of deposited WS-PPP. It should be noted that the film prepared by spin-assembly was absorbed onto only one side, while the film prepared by LBL assembly was adsorbed onto both sides of the quartz plate. Therefore, in order to compare the absorption behavior, the absorbance values of the LBL assembly were reduced by half for normalization. Figure 3 shows the normalized absorbance change at 345 nm of the UV–vis spectra measured after each bilayer assembly process. In both cases, the absorbance showed a linear increase from 1 to 15 bilayers, indicating that the imogolite and WS-PPP were successfully assembled. The film absorbance change prepared by the LBL assembly and the spin-assembly were 0.0048 and 0.0027 per bilayer, respectively.

Because of the fiber structure of imogolite, the film surface is not smooth and the film thickness is difficult to measure by ellipsometry. Direct measurement and the average thickness of the hybrid films were obtained by scratching the hybrid films

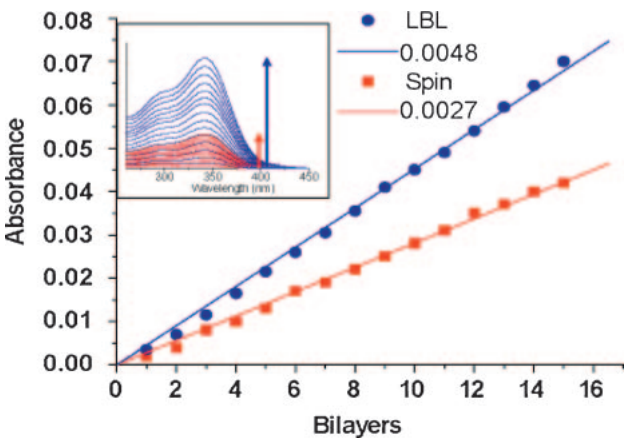

Figure 3. Increase in the absorbance at 345 nm of 15-bilayer films prepared by LBL and spin assemblies. The inset shows the UV–vis absorption spectra of WS-PPP deposited on the films. The slope implies the absorbance unit per bilayer.

on substrate with a razor blade and scanning the surface with AFM.[33] The film thickness was obtained from the height difference between the scratched substrate side and the film region. Thickness measurements were carried out at several points (more than 15 points) and the average value was calculated. Figure 4 shows that the film thickness depended on the number of deposition cycles. The thicknesses of films prepared by LBL and spin-assemblies were 2.4 and 1.7 nm/bilayer, respectively.

As indicated by the UV absorbance, the film fabricated by the LBL method adsorbed WS-PPP significantly more than that fabricated by the spin-assembly method (1.8 times higher), but, in fact, the bilayer thickness of the two films was different. This result suggests that WS-PPP can be adsorbed at higher amounts in the LBL film, resulting in a greater film thickness. If considering the present results with an equivalent thickness unit, the absorbances for films prepared by the LBL method and the spin-assembly method are 0.0020 and 0.0016 abs unit nm^{-1}, respectively. Therefore, the adsorbed amount of WS-PPP per nm for the two methods was slightly different. Even with the same molar concentration of polyelectrolytes,

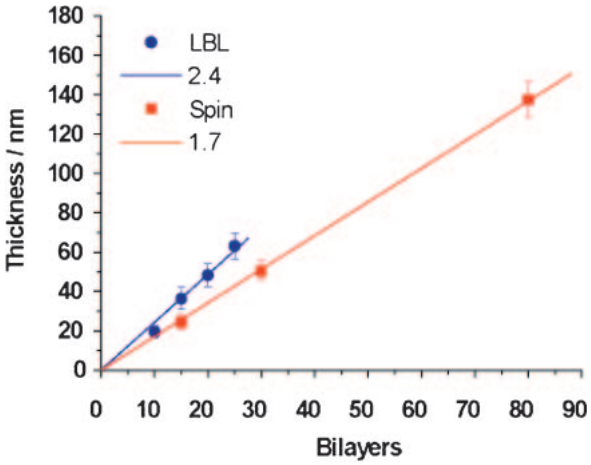

Figure 4. Thickness evaluated from AFM versus the number of bilayers of the LBL and the spin-assembly films. The slope corresponds to the thickness per bilayer.

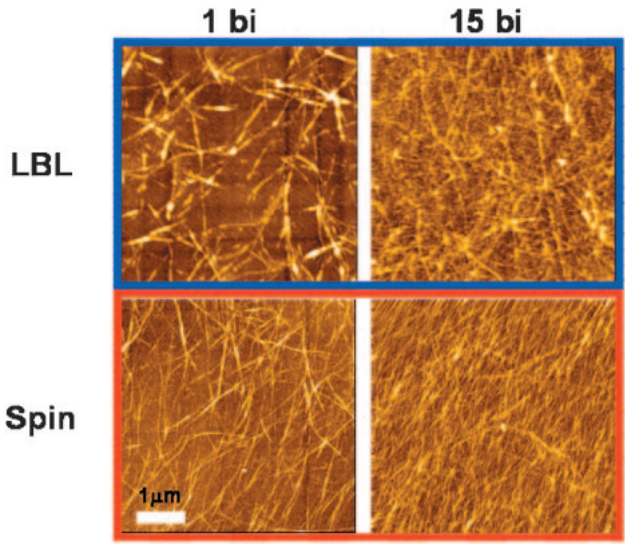

Figure 5. AFM images of 1 and 15 bilayers films prepared by the LBL and spin assemblies.

the adsorbed amount was different due to a difference in mechanism. The LBL assembly method is driven by electrostatic interactions and the adsorbed chains rearrange themselves to a near equilibrium state on the surface. In contrast, the spin-assembly method is not an equilibrium process; the adsorption is driven by electrostatic interaction, centrifugal force and air shear force.[34–37] During the spin stage, most of the excess solution is forced off the edge because of the rotation of the substrate drive. At the same time, it is important that a sufficient amount solution always remain on the substrate. The obtained results indicated that the adsorption ability in the LBL assembly process was slightly higher than that in the spin-assembly process. In contrast, previous studies[13,14,38] have found that films prepared by spin-assembly provide smoother, thicker and higher adsorption than those prepared by the LBL assembly. The reason for this difference may be attributed to a difference in the shape, mass and density of polyelectrolytes. In the present system, imogolite nanofibers with a high aspect ratio were used, although amorphous polymers or particles with a low aspect ratio have been used as polyelectrolytes in previous studies.

In the course of the AFM observation, we found that the spin-assembly had a significant effect on the planar alignment of imogolite nanofibers. Figure 5 shows AFM images of imogolite/WS-PPP hybrid films prepared by the LBL and spin-assembly methods. Very interestingly, imogolite in the spin-assembled films were oriented with a higher degree of order, while imogolite was randomly included in the LBL film. This more highly ordered structure was observed not only in the single-layer film, but also the multilayer film (15 bilayers).

In order to obtain further insight into the ordered structure of imogolite nanofibers in the hybrid films prepared by the spin-assembly method, careful AFM observation was carried out at different positions of the substrate. Importantly, as shown in Figure 6, AFM images for the spin-assembled film shows the surface morphology of imogolite nanofibers with planar alignment in a radial direction. The orientation in radial direction was due to the shear force and the centrifugal forces during the spin-assembly process. In addition, imogolite has been reported to form lyotropic liquid crystal when the concentration exceeds a certain critical point.[39,40] The LBL assembly with orderd structure of rigid rod biomacromolecules induced by liquid-crystalline behavior has been reported.[41] During the spinning process, the concentration of imogolite solution is increased by evaporation of the solvent. Simultaneously, the orientation of nanofibers in a force-induced direction may occur. The shear force and the centrifugal forces increase outward in a radial direction. In the center of the substrate, these two forces are small, so the radial alignment of imogolite did not occur. However, the evolution of radial alignment depended on the fiber size, fiber length, and solution concentration. In the case of shorter imogolite fibers, a radial orientation could not be observed under identical conditions.

In order to investigate the orientation of imogolite fibers in the spin-assembled film, polarized absorbance for the LBL and spin films were measured. Because orientation of imogolite fibers on the spin substrate varied with radial direction as shown in Figure 6, we measured in specific areas by using a 4 mm diameter slit to decrease the beam size to a given spot. Light (300–500 nm) was polarized in the direction parallel (0°) and perpendicular (90°) to rotation axis of the substrate. In Figure 7, the absorbance of the spin film depended on the area of the substrate. In the case of the edge area, $A(spin)_0$ at 345 nm was much higher than $A(spin)_{90}$ and the ratio of $A(spin)_0/A(spin)_{90}$ at 345 nm was 1.53. In contrast, in the center area, $A(spin)_0$ and $A(spin)_{90}$ were almost the same, less than 1.1. This is clearly due to the radial orientation of imogolite fibers in the same direction for the spin film and the conjugated polymer was selectively adsorbed on imogolite fibers, therefore, polarized UV absorbance of the parallel direction was higher than that in the perpendicular direction. In the case of the LBL film, $A(LBL)_0$ and $A(LBL)_{90}$ were almost the same in any position of the substrate. Actually, the absorbance of both directions was similar depending on the randomly oriented imogolite fibers on the substrate. These supporting results clearly indicated highly ordered imogolite fibers in the spin-assembled film compared with the LBL film.

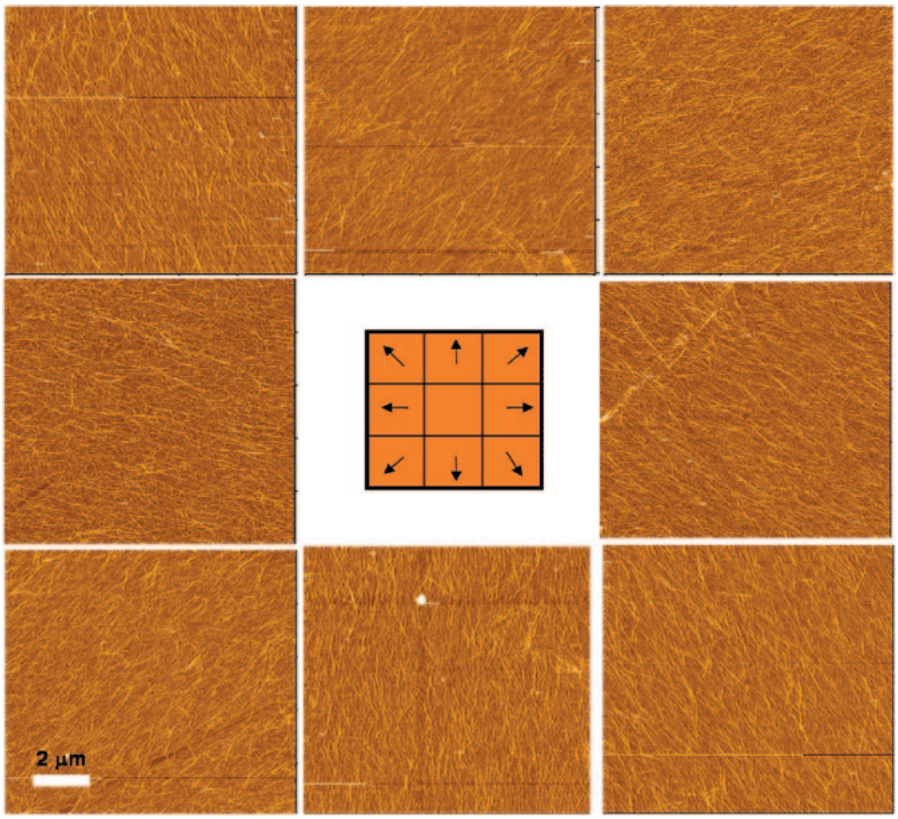

Figure 6. AFM images of imogolite nanofibers at 6000 rpm on substrate.

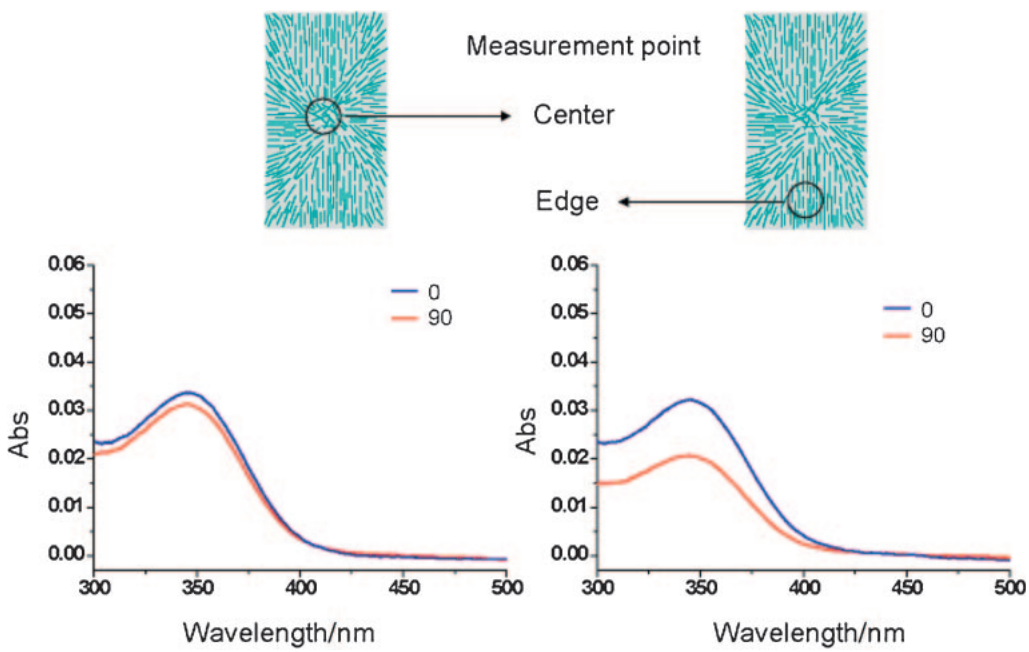

Figure 7. Schematic representation of fibers on the spin substrate and polarized UV-absorption spectra of the 15 bilayers spin film measured at center (left) and edge (right) of substrate.

Conclusion

We have demonstrated two assembly methods to fabricate hybrid multilayer films of inorganic nanofibers, imogolite and water-soluble conjugated polymer, WS-PPP. The LBL assembly and the spin-assembly of imogolite and WS-PPP were successfully performed. The deposited amounts of WS-PPP per thickness differed slightly between the two assembly methods. Interestingly, the morphology of the spin-assembled films showed a highly ordered orientation of imogolite compared

with that obtained from the conventional LBL method. That is, nanofibers showed planar alignment in a radial direction by the spin-assembly method. Imogolite nanofibers were used as templates to order conjugated polymer at the surface of nanofibers by ionic interaction. This is a simple and applicable method to prepare highly ordered hybrid film of nanofibers and conjugated polymers.

This work was supported by a Grant-in-Aid for Science Research in a Priority Area "Super-Hierarchical Structures" (Grant No. 446) from the Ministry of Education, Culture, Sports, Science and Technology, Japan. The present work is also supported by a Grant-in-Aid for the Global COE Program, "Science for Future Molecular Systems" from the Ministry of Education, Culture, Sports, Science and Technology of Japan. We thank Prof. Shin-Ichiro Wada, Faculty of Agriculture, Kyushu University, for his helpful advice regarding imogolite synthesis.

References

1 J.-D. Hong, D. Kim, K. Char, J.-I. Jin, *Synth. Met.* **1997**, *84*, 815.
2 H. Hong, R. Steitz, S. Kirstein, D. Davidov, *Adv. Mater.* **1998**, *10*, 1104.
3 H.-C. Lee, T.-W. Lee, O. O. Park, *Opt. Mater.* **2003**, *21*, 187.
4 B.-H. Sohn, T.-H. Kim, K. Char, *Langmuir* **2002**, *18*, 7770.
5 P. A. Chiarelli, M. S. Johal, D. J. Holmes, J. L. Casson, J. M. Robinson, H.-L. Wang, *Langmuir* **2002**, *18*, 168.
6 M. S. Johal, J. L. Casson, P. A. Chiarelli, D.-G. Liu, J. A. Shaw, J. M. Robinson, H.-L. Wang, *Langmuir* **2003**, *19*, 8876.
7 C. J. Lefaux, J. A. Zimberlin, A. V. Dobrynin, P. T. Mather, *J. Polym. Sci., Part B: Polym. Phys.* **2004**, *42*, 3654.
8 M. S. Johal, M. Howland, J. M. Robinson, J. L. Casson, H.-L. Wang, *Chem. Phys. Lett.* **2004**, *383*, 276.
9 M. An, J.-D. Hong, *Thin Solid Films* **2006**, *500*, 74.
10 H. Kim, J. Cho, D. Y. Kim, K. Char, *Polym. Prepr.* **2007**, *48*, 488.
11 G. Decher, J.-D. Hong, *Makromol. Chem., Macromol. Symp.* **1991**, *46*, 321.
12 G. Decher, *Science* **1997**, *277*, 1232.
13 P. A. Chiarelli, M. S. Johal, J. L. Casson, J. B. Roberts, J. M. Robinson, H.-L. Wang, *Adv. Mater.* **2001**, *13*, 1167.
14 J. Cho, K. Char, J.-D. Hong, K.-B. Lee, *Adv. Mater.* **2001**, *13*, 1076.
15 N. Yoshinaga, S. Aomine, *Soil Sci. Plant Nutr.* **1962**, *8*, 22.
16 K. Yamamoto, H. Otsuka, A. Takahara, *Polym. J.* **2007**, *39*, 1.
17 V. C. Farmer, A. R. Fraser, J. M. Tait, *J. Chem. Soc., Chem. Commun.* **1977**, 462.
18 S.-I. Wada, A. Eto, K. Wada, *J. Soil Sci.* **1979**, *30*, 347.
19 K. Yamamoto, H. Otsuka, S.-I. Wada, D. Sohn, A. Takahara, *Soft Matter* **2005**, *1*, 372.
20 W. C. Ackerman, D. M. Smith, J. C. Huling, Y. W. Kim, J. K. Bailey, C. J. Brinker, *Langmuir* **1993**, *9*, 1051.
21 S. Imamura, T. Kokubu, T. Yamashita, Y. Okamoto, K. Kajiwara, H. J. Kanai, *J. Catal.* **1996**, *160*, 137.
22 M. Suzuki, S. Suzuki, S. Tomura, M. Maeda, T. Mizota, *J. Ceram. Soc. Jpn.* **2001**, *109*, 874.
23 K. Yamamoto, H. Otsuka, A. Takahara, S.-I. Wada, *J. Adhes.* **2002**, *78*, 591.
24 F. Ohashi, S. Tomura, K. Akaku, S. Hayashi, S.-I. Wada, *J. Mater. Sci.* **2004**, *39*, 1799.
25 S. Park, Y. Lee, B. Kim, J. Lee, Y. Jeong, J. Noh, A. Takahara, D. Sohn, *Chem. Commun.* **2007**, 2917.
26 Y. Kuroda, M. Tamakoshi, J. Murakami, K. Kuroda, *J. Ceram. Soc. Jpn.* **2007**, *115*, 233.
27 H. Yang, Y. Chen, Z. Su, *Chem. Mater.* **2007**, *19*, 3087.
28 S. Kim, J. Jackiw, E. Robinson, K. S. Schanze, J. R. Reynolds, *Macromolecules* **1998**, *31*, 964.
29 T. Koga, H. Otsuka, A. Takahara, *Bull. Chem. Soc. Jpn.* **2005**, *78*, 1691.
30 T. Koga, M. Morita, H. Otsuka, A. Takahara, *Trans. Mater. Res. Soc. Jpn.* **2004**, *29*, 153.
31 S. K. Bhatia, J. L. Texeria, M. Anderson, L. C. Silverlake, J. M. Calvert, J. H. Georger, J. J. Hickman, C. S. Dulcey, P. E. Schoen, F. S. Ligler, *Anal. Biochem.* **1993**, *208*, 197.
32 H. Yonemura, Y. Yamamoto, S. Yamada, Y. Fujiwara, Y. Tanimoto, *Sci. Technol. Adv. Mater.* **2008**, *9*, 024213.
33 K. Tanaka, K. Hashimoto, T. Kajiyama, A. Takahara, *Langmuir* **2003**, *19*, 6573.
34 S. Middleman, *J. Appl. Phys.* **1987**, *62*, 2530.
35 T. J. Rehg, B. G. Higgins, *Phys. Fluids* **1988**, *31*, 1360.
36 F. Ma, J. H. Hwang, *J. Appl. Phys.* **1990**, *68*, 1265.
37 L. Cui, X. Li, Y. Han, *Appl. Surf. Sci.* **2006**, *252*, 8156.
38 S.-S. Lee, J.-D. Hong, C. H. Kim, K. Kim, J. P. Koo, K.-B. Lee, *Macromolecules* **2001**, *34*, 5358.
39 K. Kajiwara, N. Donkai, Y. Fujiyoshi, H. Inagari, *Makromol. Chem.* **1986**, *187*, 2895.
40 N. Donkai, H. Hoshino, K. Kajiwara, T. Miyamoto, *Makromol. Chem.* **1993**, *194*, 559.
41 P. J. Yoo, K. T. Nam, J. Qi, S.-K. Lee, J. Park, A. M. Belcher, P. T. Hammond, *Nat. Mater.* **2006**, *5*, 234.